EAGE

BG18

Drillbit source focusing using seismic-while drilling data in a desert environment

A. Aldawood[1], E. Hemyari[1], I. Silvestrov[1], A. Bakulin[1]

[1] Saudi Aramco

Summary

Focusing the drillbit source while-drilling can yield vital information to drillers and interpreters to help optimize their parameters and update their models. We present a case study in which we utilize a robust workflow to process seismic-while-drilling data acquired in a desert environment to image the drillbit source at its accurate subsurface positions. The results demonstrate the ability of the focusing method to localize the drillbit source as it traverses through the subsurface layers with different lithology. We modified the one-way traveltime migration kernel to allow only emanating and dip angles at the source that contains quality first arrival data to reduce the artifacts in the migrated image. We stacked all instances (images) of the sources to create a migrated image of the drillbit at all times, which showed key layers and markers associated with casing points, loss-circulation zones, major lithological changes. Identifying these markers accurately is quite useful to optimize the drilling and characterize subsurface properties.

Introduction

Locating seismic sources is essential for a wide range of geophysical applications such as earthquake location (Thurber and Engdahl, 2000), passive seismic monitoring (Shapiro, 2015), and drillbit imaging (Liu, 2021). Localizing passive sources can be achieved by inverting picked traveltimes to find the optimal location that minimizes the difference between observed and computed traveltimes (Zhang and Thurber, 2003). Traveltime picking can be erroneous for data with a low signal-to-noise ratio (SNR). To rectify this problem, waveform-based source location methods are applied to focus passive sources in their accurate subsurface positions. Time-reversal imaging aims to focus wavefields recorded by receivers at the ignition position given a reasonably accurate velocity model (Fink, 2006).

To eliminate the requirement of knowing the excitation time, waveform-based interferometric cross-correlation migration (ICCM) (Schuster et al., 2004) can be utilized to focus the passive source in the accurate subsurface position. This could be quite effective when applied to seismic-while-drilling (SWD) data acquired with continuous and random drillbit source as it drills through the different layers of the subsurface. The spatial resolution of the source image can be relatively low due to the small vertical wavenumbers obtained by imaging with a small number of recording stations placed within a limited aperture (Schuster et al., 2004). To alleviate this problem, invoking a multiplicative imaging condition instead of a cross-correlation imaging condition can suppress the migration artifacts and enhance the source image's spatial resolution (Zhu et al., 2019). Liu et al. (2021) utilized a sparsity-promoting interferometric cross-correlation migration method to enhance the spatial resolution of a focused subsurface drillbit source.

Recently, the Drilling Camera (DrillCAM) system with a 3D array of wireless receivers (~ 2,500 stations) was deployed in a desert environment to record SWD data (Bakulin et al., 2020). A wireless top-drive sensor and a memory-based downhole sensor were installed in this experiment to record the drillbit signature continuously. This abstract presents a comprehensive workflow and applies it to this recently acquired SWD data to localize the drillbit sources in the subsurface positions using a waveform-based focusing method. The objective is to obtain a robust image of the drillbit as it traverses the subsurface. We then interpret the image to resolve drilling, operational, and geological challenges.

Method

The layout of the wireless receivers in the field that continuously recorded the seismic while drilling signals is shown in Figure 1. The initial step to achieve successful retrieval of SWD data is removing the footprint of the source function (Haldorsen et al., 1995; Poletto and Miranda, 2004). Thus, the downhole sensor is the essential component of this installed system. It is used as an estimate of the source function. The recorded downhole pilot (reference) trace is utilized to deconvolve the deployed wireless receivers. This operation collapses the random, complex, and highly variable drillbit signal into an impulse-like source wavelet (Bakulin et al., 2020; Liu et al., 2021). By applying the deconvolution step, reverse vertical seismic profiling (rVSP) signals are reconstructed at each drillbit depth location (Poletto and Miranda, 2004).

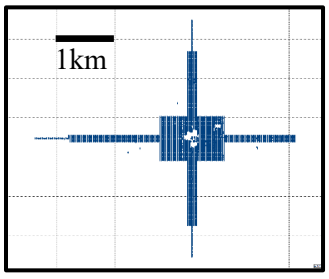

Figure 1 *The layout of the wireless receivers (blue dots) used to acquire the DrillCAM SWD data.*

We apply a stacking operation over a drilling interval of 30 ft equivalent to a single drill-pipe length to enhance the SNR of the SWD data. A combination of linear-noise removal and band-pass filter are applied to the stacked gather to mitigate the effect of surface-related noise propagating away from the

rig. Low frequencies dominate this stationary noise compared with the direct arrivals from the drillbit. Thus, high-pass filtering can be quite effective in suppressing this noise from the record (Poletto and Miranda, 2004) as shown in Figure 2. A 2D profile is extracted from the 3D geometry by combining seven East-West receiver lines using supergrouping (Bakulin et al., 2018) to further enhance the SNR acquired by the single wireless sensors, as demonstrated by Bakulin et al. (2020). As a result of the stacking operation, a 2D profile striking East-West is constructed from the 3D acquisition geometry. Subsequently, we sorted the 2D data in the common-receiver-gather (CRG) domain and applied median filtering to enhance the downgoing direct wavefields.

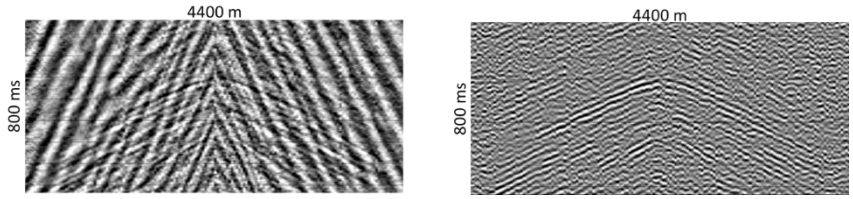

Figure 2 *A typical common-drillbit source gather before (left), and after (right) linear noise removal and high-pass filtering.*

The objective is to focus the first arrival wavefield in the accurate drillbit position; thus, we applied a mute window around the first-break (FB) picks to extract the direct arrivals, as shown in Figure 3. Then, the windowed direct wavefields are back-propagated using a depth velocity model to focus them at the source (i.e., drillbit) locations.

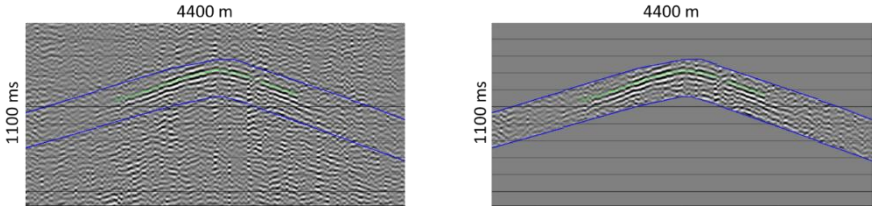

Figure 3 *A typical common-source drillbit gather with before (left) and after (right) windowing around the FB picks denoted with the green dots.*

Considering the drillbit source to be a subsurface point scatterer, the kinematic behavior of the recorded wavefield on the surface is described by one-way travel paths (Artman et al., 2010). The migrated image of the drillbit source $I(\mathbf{x})$ can be obtained in the frequency domain by the following summation of the recorded wavefield by surface receivers (Schuster et al., 2004):

$$I(\mathbf{x}) = \sum_{A,B} d(A,B) e^{-i\omega(\tau_{\mathbf{x}A} - \tau_{\mathbf{x}B})}, \quad (1)$$

where $\mathbf{x}$ is the potential position of the subsurface source. $\tau_{\mathbf{x}A}$ and $\tau_{\mathbf{x}B}$ is the traveltime from the potential drillbit position $\mathbf{x}$ to receiver A and B, respectively. $d(A,B)$ is the cross-correlated/deconvolved trace resulting from correlating the trace recorded by receiver A with the one recorded by receiver B. In simple terms, the recorded data are summed over surface defined by the one-way traveltime differences between the path from x to A, and the path from x to B as shown in schematically in Figure 4. The data is summed over all frequencies to invoke the zero-lag imaging condition of the drillbit source.

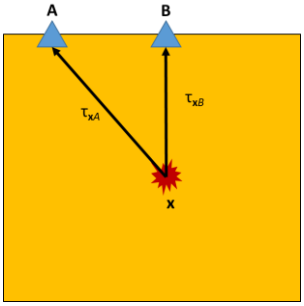

Figure 4 *A schematic figure showing the paths of one-way traveltimes between the subsurface drillbit position* **x** *and the surface receivers A and B.*

Results

In the DrillCAM experiment, a top-drive sensor was deployed to record robust drillbit source signatures continuously. The vertical component of this sensor was used as a reference receiver *B* and cross-correlated with all recording wireless receivers. Thus, we only perform the summation in equation (1) over *A*'s, which are the correlated traces recorded by the wireless geophones. The traveltimes used in the migration kernel are computed using an eikonal solver. The velocity model is constructed by inverting all available quality first-break picks along this profile and is shown in Figure 5 (left).

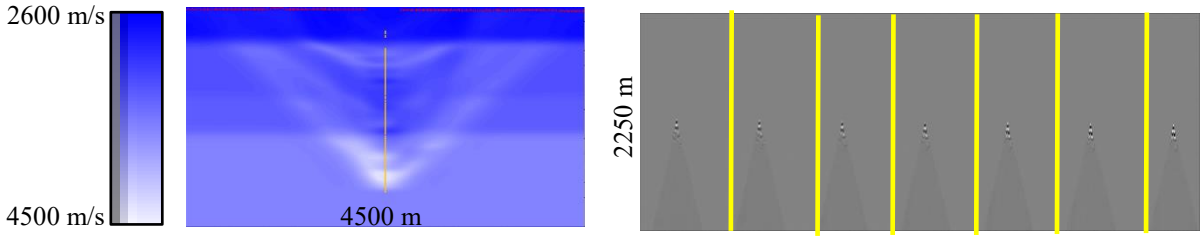

Figure 5 *The migration velocity model obtained from inverting FB picks (left) and the migrated images of several drillbit sources at different depth levels around a depth of 1 km (right).*

To mitigate the effect of the low spatial resolution of back-projection of the recorded wavefield into the model space, we restricted the migration kernel by allowing only emanating angles from the source with quality data recorded by the surface receivers and limiting the dip angles of the migrated point sources. The maximum allowed emanating angle from the source is 65 degrees, and the maximum allowed dip at the source is about 15 degrees to lessen the effect of the migration smiles. The migrated drillbit source images from different levels at around 1 km depth are shown in Figure 5 (right), and they show good focusing of the source at its accurate subsurface position. Finally, we stacked all the images from all depth instances to obtain the image that tracks the bit as it traverses through the different subsurface layers shown in Figure 6.

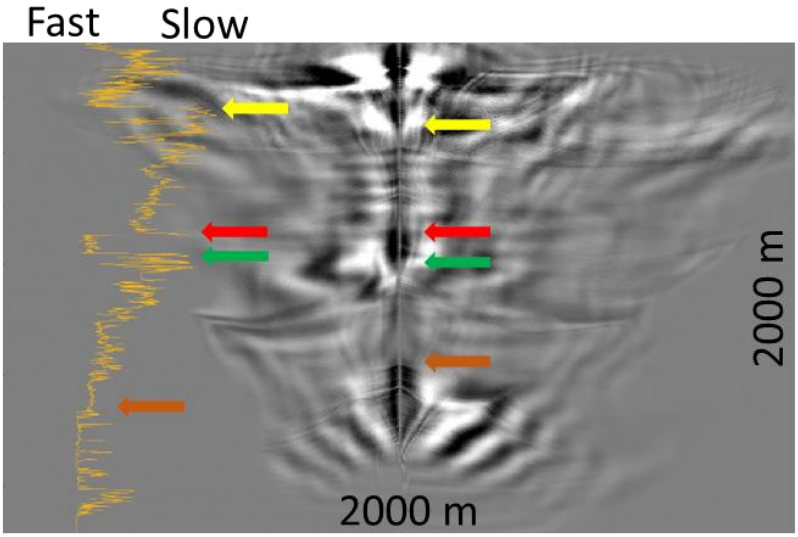

Figure 5 *The stacked migrated image from all depth instances of the drillbit overlaid by a sonic log from a neighbouring well. The arrows indicate major lithological markers associated with different drillbit signatures on the migrated section.*

We overlay the migrated image in the figure with a P-wave sonic log acquired in a representative well in this field that has been logged from the surface. This well is about 30 km away from the well where this SWD data was acquired. The shallow section shows drilling through a compacted carbonate with fast compressional velocities. The yellow arrow marks a major lithological change from compacted carbonates to a clastic rock formation consisting of interbedded shale and sand layers. Detecting this

boundary is quite essential to drillers and geologists, as it is a major casing point. A highly compacted sandstone formation shows a distinct SWD drillbit signature bounded between the red and green arrows and associated with a high compressional velocity. Delineating the top and bottom of this layer is crucial, as drilling through transitions into and out of this layer requires careful optimization of drilling parameters, mainly mud weights, since loss-circulations are often encountered near this zone. The formations between the green and brown arrows mainly consists of porous clastic rocks and soft carbonates, resulting in a quieter drillbit signature. The last critical formation top pointed by the brown arrow marks a thick layer of highly compacted anhydrite, associated with fast sonic velocities. Drilling through this compacted anhydrite gives a distinct change in the drillbit signature in Figure 5.
Note that the thicknesses of the different formations may vary between the logged well and the SWD well; however, the regional markers are quite distinct and were subsequently confirmed by the drilling cutting samples.

Conclusions

We presented a processing workflow to localize a drillbit source in its accurate subsurface positions acquired with a wireless and synchronised SWD system. The initial steps of the workflow aimed to enhance the SNR of the low-quality drillbit source data. The first arrivals were subsequently windowed and input to a back-projection algorithm to localize the drillbit source at all instances. To eliminate the artefacts arising from the back-projection, we customized the source imaging kernels to allow emanating and dip angles at the source. The images of the sources were then stacked together to obtain a migrated image with all source instances as it traverses through different layers. We then interpreted the results and noted markers associated with a casing point, a loss-circulation zone, and other key markers that give distinct drillbit signatures. We demonstrated how seismic recordings while drilling could provide vital real-time information to drillers and geoscientists to optimize the drilling operation and update their subsurface models.

References

Artman, B., Podladtchikov, I., and Witten, B. [2010] Source location using time-reverse imaging. *Geophysical Prospecting*, **58**, 861–873

Bakulin, A., Golikov, P., Dmitriev, M., Neklyudov, D., Leger, P. and Dolgov, V. [2018] Application of supergrouping to enhance 3D prestack seismic data from a desert environment. *The Leading Edge*, **37** (3), 200-207.

Bakulin, A., Aldawood, A., Silvestrov, I., Hemyari, E. and Poletto, F. [2020] Seismic-while-drilling applications from the first DrillCAM trial with wireless geophones and instrumented top drive. *The Leading Edge*, **39**(6), pp.422-429.

Fink, M. [2006] Time-reversal acoustics in complex environments: *Geophysics*, **71**, no. 4, SI151-SI164

Haldorsen, J.B., Miller, D.E. and Walsh, J.J. [1995] Walk-away VSP using drill noise as a source. *Geophysics*, **60**(4), pp.978-997.

Liu, Y., Du, Y. and Luo, Y. [2021] Sparsity-promoting least-squares interferometric migration for high-resolution passive source location. *Geophysics*, **86**(1), pp.KS1-KS9.

Poletto, F., and Miranda, F. [2004] *Seismic while drilling: Fundamentals of drillbit seismic for exploration*. Elsevier, 35

Shapiro, S. [2015] *Fluid-induced micro seismicity*. Cambridge University Press.

Schuster, G.T., Yu, J., Sheng, J., and Rickett, J. [2004] Interferometric/daylight seismic imaging. *Geophysical Journal International*, **157**, 838–852

Thurber, C. H., and Engdahl, E. R. [2000] Advances in global seismic event location. *in Advances in seismic event location.* Springer, 3-22.

Zhang, H., and Thurber, C. H. [2003] Double-difference tomography: The method and its application to the Hayward Fault, California. *Bulletin of the Seismological Society of America*, **93**, 1875-1889

Zhu, T., Sun, J., Gei, D., Carcione, J.M., Cance, P., and Huang, C. [2019] Hybrid multiplicative time-reversal imaging reveals the evolution of microseismic events: Theory and field-data tests: *Geophysics*, **84**, no. 3, KS71-KS83